Journal of Communication, Navigation and Signal Processing (January 2012)
Vol. 1, No. 1, pp. 35-45

Discrete Cosine Transform based Image Fusion Techniques

VPS Naidu

MSDF Lab, FMCD, National Aerospace Laboratories, Bangalore, INDIA
E.mail: vpsnaidu@gmail.com

Abstract: ***Six different types of image fusion algorithms based on discrete cosine transform (DCT) were developed and their performance was evaluated. Fusion performance is not good while using the algorithms with block size less than 8x8 and also the block size equivalent to the image size itself. DCTe and DCTmx based image fusion algorithms performed well. These algorithms are very simple and might be suitable for real time applications.***

Keywords: DCT, Contrast measure, Image fusion

I. INTRODUCTION

Off late, different image fusion algorithms have been developed to merge the multiple images into a single image that contain all useful information. Pixel averaging of the source images (the images to be fused) is the simplest image fusion technique and it often produces undesirable side effects in the fused image including reduced contrast. To overcome this side effects many researchers have developed multi resolution [1-3], multi scale [4,5] and statistical signal processing [6,7] based image fusion techniques.

In similar line, contrast based image fusion algorithm in DCT domain has been presented [8] to fuse the out of focus images. Local contrast is measured by 8x8 blocks. However, there is no discussion on the fusion performance by choosing different block sizes. The present paper presents six different DCT based image fusion techniques and studies their performance.

II. DISCRETE COSINE TRANSFORM

Discrete cosine transform (DCT) is an important transform extensively used in digital image processing. Large DCT coefficients are concentrated in the low frequency region; hence, it is known to have excellent energy compactness properties [9-11]. The 2D discrete cosine transform $X(k_1,k_2)$ of an image or 2D signal $x(n_1,n_2)$ of size $N_1 \text{x} N_2$ is defined as [12-14]:

$$X(k_1,k_2) = \alpha(k_1)\alpha(k_2) \sum_{n_1=0}^{N_1-1}\sum_{n_2=0}^{N_2-1} x(n_1,n_2)\cos\left(\frac{\pi(2n_1+1)k_1}{2N_1}\right) \cos\left(\frac{\pi(2n_2+1)k_2}{2N_2}\right), \quad \begin{matrix} 0 \le k_1 \le N_1-1 \\ 0 \le k_2 \le N_2-1 \end{matrix} \tag{1}$$

Where $\alpha(k_1) = \begin{cases} \frac{1}{\sqrt{N_1}}, & k_1 = 0 \\ \sqrt{\frac{2}{N_1}}, & 1 \le k_1 \le N_1-1 \end{cases}$ and

$\alpha(k_1) = \begin{cases} \frac{1}{\sqrt{N_2}}, & k_2 = 0 \\ \sqrt{\frac{2}{N_2}}, & 1 \le k_2 \le N_2-1 \end{cases}$

k_1 & k_2 discrete frequency variables (n_1,n_2) pixel index

Similarly, the 2D inverse discrete cosine transform is defined as:

$$x(n_1,n_2) = \alpha(k_1)\alpha(k_2) \sum_{k_1=0}^{N_1-1}\sum_{k_2=0}^{N_2-1} \alpha(k_1)\alpha(k_2)X(k_1,k_2)\cos\left(\frac{\pi(2n_1+1)k_1}{2N_1}\right) \cos\left(\frac{\pi(2n_2+1)k_2}{2N_2}\right), \quad \begin{matrix} 0 \le n_1 \le N_1-1 \\ 0 \le n_2 \le N_2-1 \end{matrix} \tag{2}$$

III. CONTRAST MEASURE

DCT decomposes the image/block into a series of waveforms, each with a particular frequency. DCT coefficients are segregated into $2N-1$ different frequency bands for image or block of size NxN . The m^{th} band is composed of the coefficients with $m = k_1 + k_2$. The contrast measure at each coefficient in m^{th} the band is computed as [15-17]:

$$C(k_1,k_2) = \frac{X(k_1,k_2)}{\sum_{j=0}^{m-1} E_j} \tag{3}$$

Where $E_j = \frac{\sum_{j=t+p} |X(p,t)|}{Y}$ and $Y = \begin{cases} j+1 & j < N \\ 2(N-1)-j+1 & j \ge N \end{cases}$ (4)

E_j is the average amplitude over a j^{th} spectral band. The DCT output for image or block size of 8x8 is shown in Fig-1. It also illustrates the 1st and 5th bands (enclosed with rectangles).

$$X = \begin{bmatrix} X(0,0) & X(0,1) & X(0,2) & X(0,3) & X(0,4) & X(0,5) & X(0,6) & X(0,7) \\ X(1,0) & X(1,1) & X(1,2) & X(1,3) & X(1,4) & X(1,5) & X(1,6) & X(1,7) \\ X(2,0) & X(2,1) & X(2,2) & X(2,3) & X(2,4) & X(2,5) & X(2,6) & X(2,7) \\ X(3,0) & X(3,1) & X(3,2) & X(3,3) & X(3,4) & X(3,5) & X(3,6) & X(3,7) \\ X(4,0) & X(4,1) & X(4,2) & X(4,3) & X(4,4) & X(4,5) & X(4,6) & X(4,7) \\ X(5,0) & X(5,1) & X(5,2) & X(5,3) & X(5,4) & X(5,5) & X(5,6) & X(5,7) \\ X(6,0) & X(6,1) & X(6,2) & X(6,3) & X(6,4) & X(6,5) & X(6,6) & X(6,7) \\ X(7,0) & X(7,1) & X(7,2) & X(7,3) & X(7,4) & X(7,5) & X(7,6) & X(7,7) \end{bmatrix}$$

Fig-1 DCT output of an image or a bock size of 8x8

IV. IMAGE FUSION

Six different types of image fusion techniques using DCT are presented in this section. Image to be fused are divided into non-overlapping blocks of size NxN as shown in Fig-2. DCT coefficients are computed for each block and fusion rules are applied to get fused DCT coefficients. IDCT is then applied on the fused coefficients to produce the fused image/block. The procedure is repeated for each block.

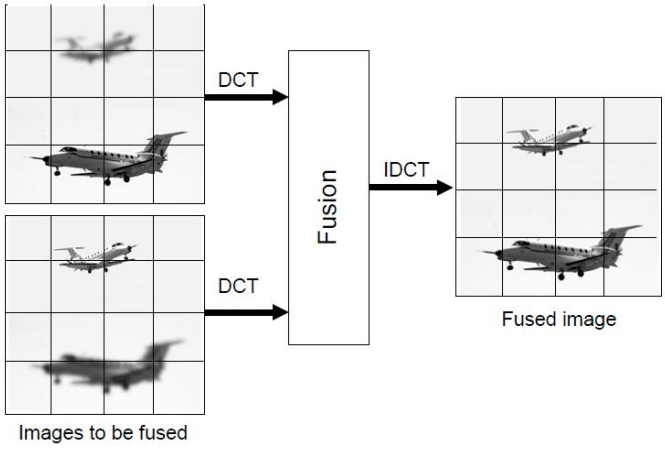

Fig-2 Framework of DCT based image fusion algorithm

The following fusion rules are used in image fusion process. Let the X_1 be the DCT coefficients of image block from image I_1 and similarly let the X_2 be the DCT coefficients of image block from image I_2. Assume the image block is of size NxN and X_f be the fused DCT coefficients.

DCT av: In this fusion rule, all DCT coefficients from both image blocks are averaged to get fused DCT coefficients. It is very simple and basic image fusion technique in DCT domain.

$$X_f(k_1,k_2) = 0.5\ X_1(k_1,k_2) + X_2(k_1,k_2) \quad (5)$$

Where $k_1,k_2 = 0,1,2,\ldots,N-1$

DCTma: The DC components from both image blocks are averaged. The largest magnitude AC coefficients are chosen, since the detailed coeficients correspond to sharper brightness changes in the images such as edges and object boundaries etc. These coeficients are fluctuating around zero.

$$X_f(0,0) = 0.5\ X_1(0,0) + X_2(0,0) \quad (6a)$$

$$X_f(k_1,k_2) = \begin{cases} X_1(k_1,k_2) & |X_1(k_1,k_2)| \geq |X_2(k_1,k_2)| \\ X_2(k_1,k_2) & |X_1(k_1,k_2)| < |X_2(k_1,k_2)| \end{cases} \quad (6b)$$

Where $k_1,k_2 = 1,2,3,\ldots,N-1$

DCTah: The lowest AC components including DC coefficients are averaged and the remaining AC coefficients are chosen based on largest magnitude.

$$X_f(k_1,k_2) = 0.5\ X_1(k_1,k_2) + X_2(k_1,k_2) \quad (7a)$$

Where $k_1,k_2 = 0,1,2,\ldots,0.5N-1$

$$X_f(k_1,k_2) = \begin{cases} X_1(k_1,k_2) & |X_1(k_1,k_2)| \geq |X_2(k_1,k_2)| \\ X_2(k_1,k_2) & |X_1(k_1,k_2)| < |X_2(k_1,k_2)| \end{cases} \quad (7b)$$

Where $k_1,k_2 = 0.5N, 0.5+1, 0.5N+2,\ldots,N-1$

DCTcm: The DC coefficients are averaged and the AC coefficients are chosen based on largest contrast measure.

$$X_f(0,0) = 0.5\ X_1(0,0) + X_2(0,0) \quad (8a)$$

$$X_f(k_1,k_2) = \begin{cases} X_1(k_1,k_2) & C_1(k_1,k_2) \geq C_2(k_1,k_2) \\ X_2(k_1,k_2) & C_1(k_1,k_2) < C_2(k_1,k_2) \end{cases} \quad (8b)$$

Where $k_1,k_2 = 1,2,3,\ldots,N-1$

DCTch: It is very much similar to DCT ah. The lowest AC components including DC coefficients are averaged and the remaining AC coefficients are chosen based on largest contrast measure.

$$X_f(k_1,k_2) = 0.5\ X_1(k_1,k_2) + X_2(k_1,k_2) \quad (9a)$$

Where $k_1,k_2 = 0,1,2,\ldots,0.5N-1$

$$X_f(k_1,k_2) = \begin{cases} X_1(k_1,k_2) & C_1(k_1,k_2) \geq C_2(k_1,k_2) \\ X_2(k_1,k_2) & C_1(k_1,k_2) < C_2(k_1,k_2) \end{cases} \quad (9b)$$

Where $k_1,k_2 = 0.5N, 0.5+1, 0.5N+2, \ldots, N-1$

DCTe: It is similar to DCTcm. DC components are averaged together. AC coefficients correspond to the frequency band having largest energy is chosen.

$$X_f(0,0) = 0.5\ X_1(0,0) + X_2(0,0) \quad (10a)$$

$$X_f(k_1,k_2) = \begin{cases} X_1(k_1,k_2) & E_{j1} \geq E_{j2} \\ X_2(k_1,k_2) & E_{j1} < E_{j2} \end{cases} \quad (10b)$$

Where $k_1,k_2 = 1,2,3,\ldots,N-1$ and $j = k_1 + k_2$

V. Fusion Evaluation Metrics

The following fusion evaluation metrics are used to evaluate the performance of the developed six image fusion algorithms. When the ground truth image is available:

1. Peak Signal to Noise Ratio (PSNR) [3,6,18]
   PSNR value will be high when the fused and the ground truth images are comparable. Higher value implies better fusion. The peak signal to noise ratio is computed as:

$$PSNR = 20\log_{10}\left(\frac{L^2}{\frac{1}{MN}\sum_{i=1}^{M}\sum_{j=1}^{N}\left(I_r(i,j) - I_f(i,j)\right)^2}\right) \quad (11)$$

Where L in the number of gray levels in the image

2. Structural Similarity (SSIM) Index [19,20]

It is a method for measuring the similarity between the fused and reference images. Its value may vary from -1 to 1. The value 1 implies that both images are identical. The fused image with high SSIM would be considered. The SSIM is computed as:

$$SSIM(I_t,I_f) = \frac{2\mu_{I_t}\mu_{I_f} + c_1 \quad 2\sigma_{I_t I_f} + c_2}{\mu_{I_t}^2 + \mu_{I_f}^2 + c_1 \quad \sigma_{I_t}^2 + \sigma_{I_f}^2 + c_2} \quad (12)$$

Where μ_{I_t} : mean of I_t

μ_{I_f} : mean of I_f

$\sigma_{I_t}^2$: Variance of I_t

$\sigma_{I_f}^2$: Variance of I_f

$\sigma_{I_t I_f}$: Covariance of I_f and I_t

$c_1 = (0.01L)^2$ and $c_3 = (0.03L)^2$ are the constants to stabilize the division with weak denominator

When the ground truth image is not available, the following metrics can be used to evaluate the proposed six fusion algorithms.

1. Spatial Frequency [6,21]
   The frequency in spatial domain indicates the overall activity level in the fused image and it is computed as

Row frequency:

$$RF = \sqrt{\frac{1}{MN}\sum_{i=0}^{M-1}\sum_{j=1}^{N-1}\left(I_f(i,j) - I_f(i,j-1)\right)^2} \quad (13a)$$

Column frequency:

$$CF = \sqrt{\frac{1}{MN}\sum_{j=0}^{N-1}\sum_{i=1}^{M-1}\left(I_f(i,j) - I_f(i-1,j)\right)^2} \quad (13b)$$

Spatial frequency: $SF = \sqrt{RF^2 + CF^2}$ (14)

The fused image with high SF would be considered.

2. Fusion quality index [22]

The range of this metric is 0 to 1. One indicates the fused image contains all the information from the source images.

$$FQI = \sum_{w \in W} c(w)\left(\lambda(w)QI(I_1,I_f \mid w) + (1-\lambda(w))QI(I_2,I_f \mid w)\right) \quad (15)$$

Where $\lambda(w) = \frac{\sigma_{I_1}^2}{\sigma_{I_1}^2 + \sigma_{I_2}^2}$ computed over a window

$C(w) = \max\left(\sigma_{I_1}^2, \sigma_{I_2}^2\right)$ Over a window

$c(w)$ is a normalized version of $C(w)$

$QI(I_1,I_f \mid w)$ is the quality index over a window for a given source image and fused image

VI. Results and Discussions

The ground truth image I_t (SARAS) is shown in Fig-3. The complementary source images I_1 & I_2 (images to be fused) are generated by blurring the source image as shown in Fig-4. The fused and the error images using the developed image fusion techniques are shown in Fig-5 to Fig-10. The error image is the

difference of ground truth and the fused images. It is observed from the error image (Fig-5) that DCTav image fusion algorithm has not performed well. There is information less at edges. DCTmx performed better than DCTav. DCTah is not performed well. There is information loss at the edges and some ringing tones are observed at the sharp edges as shown in Fig-7. Image fusion by contrast measure (DCTcm) performed well compare to the previous techniques. DCTch is not producing good results. It is almost similar to DCTah and same observations are made. The algorithm DCTe provides superior fusion results among all fusion techniques. It is computationally simplest fusion algorithm compare to DCTcm and DCTch. The fusion quality evaluation metrics are shown in Table-1 and 2. It is observed that DCTe performed very well followed by DCTcm and DCTmx.

Fig-3 Ground truth image - SARAS

Fig-4 Source images for image fusion - SARAS

Fig-5 The fused and error image using DCTav fusion algorithm - SARAS

Table-1a Peak signal to noise ratio – SARAS

	Block size (rows x columns)								
	2x2	4x4	8x8	16x16	32x32	64x64	128x128	256x256	512x512
DCTav	38.4255	38.4255	38.4255	38.4255	38.4255	38.4255	38.4255	38.4255	38.4255
DCTmx	38.8067	39.6028	40.7588	42.0532	43.5130	44.6817	45.8894	53.7908	39.3178
DCTah	38.8067	38.7442	38.6715	38.6400	38.6225	38.6140	38.6089	38.6051	38.4843
DCTe	38.8073	39.6142	40.7857	42.1961	43.7510	45.2481	47.1747	**61.4135**	37.6962
DCTch	38.8098	38.7442	38.6715	38.6400	38.6225	38.6140	38.6089	38.6051	38.4842
DCTcm	38.8098	39.6152	40.7970	42.0552	43.5079	44.6773	45.8894	53.7829	39.3171

Table-1b Structural similarity index – SARAS

	Block size (rows x columns)								
	2x2	4x4	8x8	16x16	32x32	64x64	128x128	256x256	512x512
DCTav	0.9821	0.9821	0.9821	0.9821	0.9821	0.9821	0.9821	0.9821	0.9821
DCTmx	0.9741	0.9760	0.9753	0.9815	0.9911	0.9941	0.9967	0.9998	0.7624
DCTah	0.9741	0.9738	0.9719	0.9706	0.9695	0.9687	0.9680	0.9674	0.9238
DCTe	0.9740	0.9760	0.9755	0.9826	0.9924	0.9965	0.9987	**1.0000**	0.9121
DCTch	0.9740	0.9737	0.9719	0.9706	0.9695	0.9687	0.9680	0.9674	0.9237
DCTcm	0.9740	0.9760	0.9751	0.9814	0.9910	0.9940	0.9967	0.9998	0.7616

Table-2a spatial frequency – SARAS

	Block size (rows x columns)								
	2x2	4x4	8x8	16x16	32x32	64x64	128x128	256x256	512x512
DCTav	9.1266	9.1266	9.1266	9.1266	9.1266	9.1266	9.1266	9.1266	9.1266
DCTmx	13.8784	16.3318	16.9361	16.9999	16.9693	16.9825	16.9741	16.9952	15.5576
DCTah	13.8784	13.4645	13.0127	12.7814	12.6372	12.5612	12.5096	12.4763	11.8111
DCTe	13.8809	16.3323	16.9222	16.9795	16.9738	16.9808	16.9915	**17.0003**	13.1844
DCTch	13.8833	13.4647	13.0127	12.7813	12.6371	12.5612	12.5096	12.4763	11.8109
DCTcm	13.8833	16.3286	16.9323	16.9977	16.9703	16.9826	16.9741	16.9952	15.5574

Table-2b Fusion quality index – SARAS

	Block size (rows x columns)								
	2x2	4x4	8x8	16x16	32x32	64x64	128x128	256x256	512x512
DCTav	0.7466	0.8560	0.7470	0.8560	0.7576	0.8560	0.7700	0.8565	0.8059
DCTmx	0.7888	**0.8950**	0.8081	0.8890	0.8041	0.8423	0.7495	0.8012	0.6425
DCTah	0.7888	0.8843	0.7893	0.8709	0.7917	0.8354	0.7729	0.7591	0.5576
DCTe	0.7883	0.8940	0.8067	0.8861	0.7955	0.8455	0.7862	0.8496	0.5270
DCTch	0.7886	0.8843	0.7892	0.8709	0.7917	0.8353	0.7728	0.7590	0.5574
DCTcm	0.7886	0.8949	0.8081	0.8892	0.8042	0.8423	0.7492	0.8011	0.6438

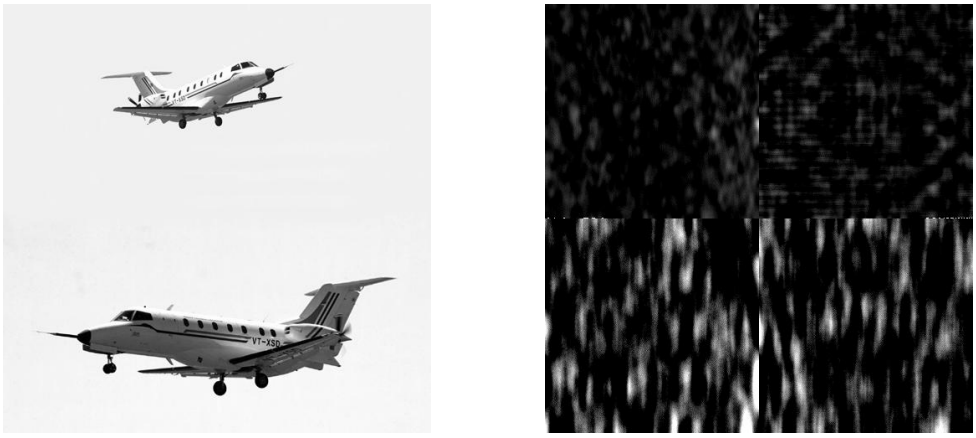

Fig-6 The fused and error image using DCTmx fusion algorithm - SARAS

Fig-7 The fused and error image using DCTah fusion algorithm – SARAS

Fig-8 The fused and error image using DCTe fusion algorithm - SARAS

Fig-9 The fused and error image using DCTch fusion algorithm - SARAS

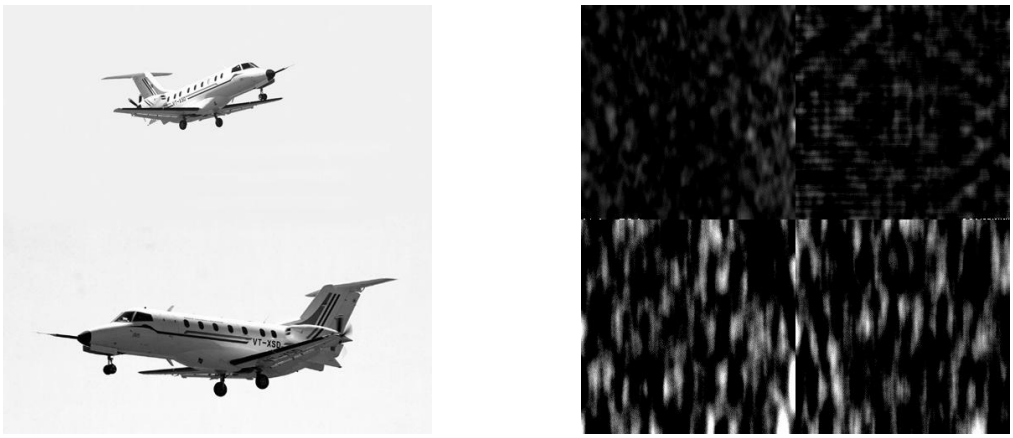

Fig-10The fused and error image using DCTcm fusion algorithm - SARAS

The computational time taken by each fusion algorithm with chosen block size are shown in Table-3 and Fig-11. It is observed that the algorithm with block size less than 8x8 takes more time and performance is also not good. DCTmx takes very less time and produces almost similar results compared to DCTe and DCTcm.

Table-3 Computational time in sec.

	Block size (rows x columns)								
	2x2	4x4	8x8	16x16	32x32	64x64	128x128	256x256	512x512
DCTav	22.6578	5.9152	1.5946	0.4896	0.1859	0.1617	**0.1085**	0.2009	0.2738
DCTmx	23.1537	6.0213	1.6209	0.4881	0.1886	0.1691	0.1164	0.2028	0.2831
DCTah	23.7942	6.1585	1.6665	0.5042	0.1988	0.1665	0.1226	0.2065	0.2847
DCTe	34.4017	11.9302	4.8228	2.3368	1.4845	1.4178	1.8222	4.2950	9.7422
DCTch	38.1772	13.9753	6.3237	3.6836	2.8434	2.8650	3.3388	6.2736	12.2554
DCTcm	37.5996	13.8168	6.2946	3.6875	2.8610	2.8832	3.3556	7.2242	12.2676

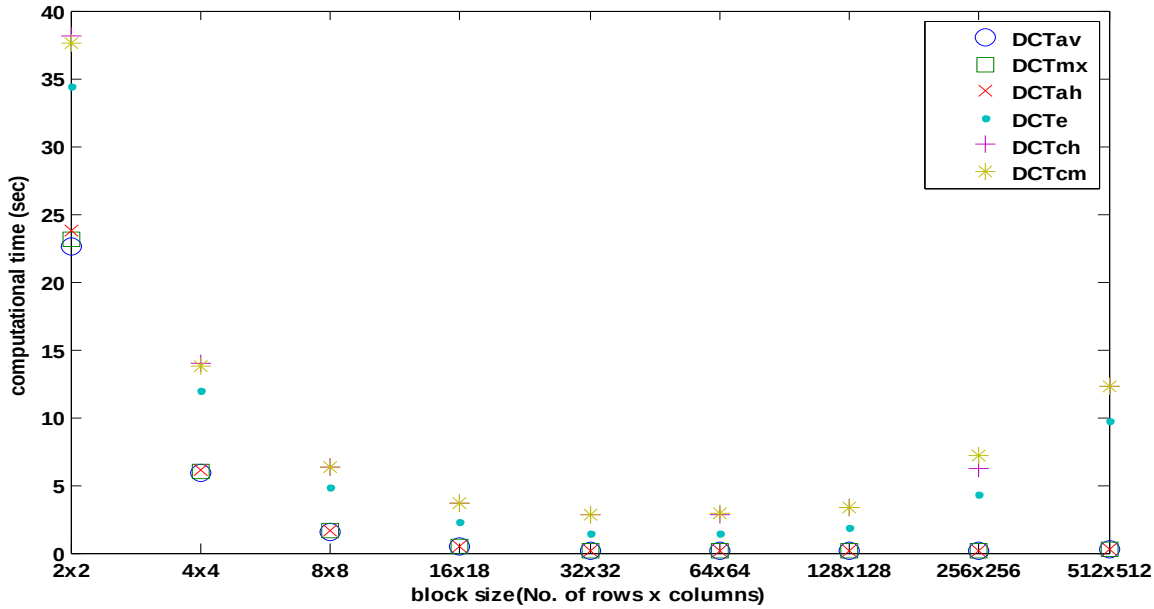

Fig-11 Computational time for different types of DCT based image fusion algorithms

The algorithms are applied on the second set of images (lab) obtained from [23] as shown in Fig-12. Both the images are out of focus. The first image is focused on right half where the time piece visible clearly. The second image is focused on left half where the book self and other things visible clearly. The fused images using the developed fusion techniques are shown in Fig-13 and 14. The fused image is focused everywhere. The fusion quality evaluation metrics are shown in Table-4. Similar observation as earlier can be made here also.

Fig-12 Images to be fused - lab

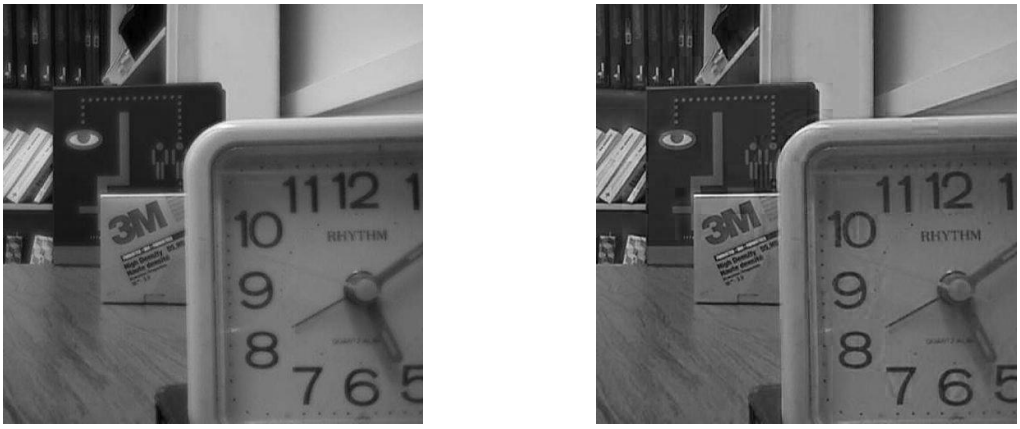

Fig-13 Fused images using DCTav and DCTmx

Fig-14 Fused images using DCTe and DCTcm

Table-4a Spatial frequency – lab

	Block size (rows x columns)								
	2x2	4x4	8x8	16x16	32x32	64x64	128x128	256x256	512x512
DCTav	7.3952	7.3952	7.3952	7.3952	7.3952	7.3952	7.3952	7.3952	7.3952
DCTmx	10.1993	12.2656	12.8763	13.0599	13.0847	**13.0931**	13.0332	12.8867	12.4514
DCTah	10.1993	9.6076	8.9455	8.6306	8.6040	8.5611	8.5590	8.5245	8.4466
DCTe	10.1947	12.2373	12.8162	12.9454	12.9226	12.8466	12.6944	12.4465	11.5509
DCTch	10.1968	9.6071	8.9436	8.6296	8.6037	8.5609	8.5588	8.5240	8.4463
DCTcm	10.1968	12.2745	12.8819	13.0621	13.0847	13.0910	13.0330	12.8863	12.4507

Table-4b Fusion quality index – lab

	Block size (rows x columns)								
	2x2	4x4	8x8	16x16	32x32	64x64	128x128	256x256	512x512
DCTav	0.8045	0.8053	0.8046	0.8053	**0.8059**	0.8053	0.8045	0.8048	0.8043
DCTmx	0.7962	0.7842	0.7711	0.7564	0.7428	0.7305	0.7221	0.7027	0.6673
DCTah	0.7962	0.7842	0.7711	0.7564	0.7428	0.7305	0.7221	0.7027	0.6673
DCTe	0.7954	0.7817	0.7674	0.7484	0.7335	0.7237	0.7285	0.7190	0.6549
DCTch	0.7962	0.7997	0.7997	0.7942	0.7879	0.7825	0.7774	0.7701	0.7549
DCTcm	0.7962	0.7842	0.7708	0.7559	0.7427	0.7302	0.7218	0.7022	0.6671

From the results, it is observed that DCTe and DCTmx based image fusion algorithms would provide good fused image and these could be suitable for real time applications. Fusion performance is not good while using the algorithms with block size is less than 8x8 and also the block size equivalent to the image size itself. Fusion quality is very much depends on chosen block size and selection of block size is very difficult in practice. One way to obtain best fused image is, compute the performance of the fusion for different block sizes and then select the fused image corresponding to best performance metrics. Since very high computational facility is available, it could be possible to implement this idea for real time applications.

VII. CONCLUSION

Six different types of image fusion algorithms based on discrete cosine transform (DCT) were developed and fused image quality was evaluated using performance evaluation metrics. Fusion performance is not good while using the algorithms with block size less than 8x8 and also the block size equivalent to the image size itself. DCTe and DCTmx based image fusion algorithms performed well and these algorithms are very suitable for real time applications.

REFERENCES

[1] Gonzalo Pajares and Jesus Manuel de la Cruz, "A wavelet-based image fusion tutorial", Pattern Recognition, 37, 2007, pp.1855-1872.

[2] H. Li, B.S. Manjunath and S.K. Mitra, "Multisensor image fusion using wavelet fransform", Graph. Models Image Process, 57(3), pp.235-245, 1995.

[3] VPS Naidu, "Discrete Cosine Transform-based Image Fusion", Special Issue on Mobile Intelligent Autonomous System, Defence Science Journal, Vol. 60, No.1, pp.48-54, Jan. 2010.

[4] B. Ajazzi, L. Alparone, S. Baronti and R. Carla, "Assessment pyramid-based multisensor image data fusion", Proc. SPIE 3500, pp.237-248, 1998.
[5] Akerman, "Pyramid techniques for multisensory fusion", Proc. SPIE 2828, pp.124-131, 1992.
[6] VPS Naidu and J.R. Raol, "Fusion of Out Of Focus Images using Principal Component Analysis and Spatial Frequency", Journal of Aerospace Sciences and Technologies, Vol. 60, No. 3, pp.216-225, Aug. 2008.
[7] Rick S. Blum, "Robust image fusion using a statistical signal processing approach", Information Fusion, 6(2), pp.119-128, 2005.
[8] Jinshan Tang, "A Contrast based Image Fusion Technique in the DCT Domain", Digital Signal Processing, Vol. 14, pp.218-226, 2004.
[9] N. Ahmed, T. Natarajan and K.R.Rao, "Discrete Cosine Transform", IEEE Trans. On Computers, Vol.32, pp.90-93, 1974.
[10] Discrete Cosine Transform, http:/documents.wolfram.com/applications/digital image/ Users Guide/Image Transform/ImageProcessing8.2.html.
[11] Vassil Dimitrov and Khan Wahid, "Multiplier less DCT Algorithm for Image Compression Applications", International Journal on Information Theories and Applications, Vol.11, pp.162-169, 2004.
[12] R.C. Gonzalez and P. Wintz, "Digital Image Processing", MA: Addison-Wesley, 1987.
[13] Syed Ali Khayam, "Lecture Notes: ECE802-602-Information theory and Coding", March 2003.
[14] G. Strang, "The Discrete Cosine Transform", SIAM Review, Vol.41, pp.135-147, 1999.
[15] Jinshan Tang, Eli Peli and Scott Acton, "Image Enhancement using a Contrast Measure in the Compressed Domain", IEEE Signal Processing Letters, Vo. 10, No,10, pp. 289-292, Oct. 2003. Qingling Sun and Jinshan Tang, "A New Contrast Measure based Image Enhancement Algorithm in the DCT Domain", IEEE Systems Man and Cybernatics, Vol.3, pp.2055-2058,2003.
[16] Jinshan Tang, "A Contrast based Image Technique in the DCT Domain", Digital Signal Processing, Vol.14, pp.218-226,2004.
[17] Gonzalo R. Arce, "Nonlinear Signal Processing – A statistical approach", Wiley-Interscience Inc., Publication, USA, 2005.
[18] http://en.wikipedia.org/wiki/Structural_similarity
[19] Z. Wang, A. C. Bovik, H. R. Sheikh and E. P. Simoncelli, "Image quality assessment: From error visibility to structural similarity," IEEE Transactions on Image Processing, vol. 13, no. 4, pp. 600-612, 2004.
[20] Shutao Li, James T. Kwok and Yaonan Wang, "Combination of images with diverse focuses using the spatial frequency", Information Fusion, Vol. 2, pp. 169-176, 2001.
[21] Gemma Piella and Henk Heijmans, "A New Quality Metric for Image Fusion", Proc. IEEE International Conference on Image Processing, Barcelona, Spain, pp173-176, 2003.
[22] http://www.ece.lehigh.edu/SPCRL/IF/disk.htm

VPS Naidu obtained M.E in Medical electronics from Anna University Chennai and PhD from University of Mysore, Mysore in board of studies, Electronics. He is working at Multi sensor data fusion lab, National Aerospace Laboratories, Bangalore as scientist since December 2001. His areas of interest are: Multi Sensor Data Fusion and Enhanced Flight Vision System. He received four awards for his research contribution. He has more than fifty papers and forty-five technical reports. He is actively involved in student project programme organized by Karnataka state council for science and technology (KSCST) from 2007.